Analysis of Arabidopsis *glucose insensitive growth* Mutants Reveals the Involvement of the Plastidial Copper Transporter PAA1 in Glucose-Induced Intracellular Signaling[1][W][OA]

Shin Ae Lee, Eun Kyung Yoon, Jung-Ok Heo, Mi-Hyun Lee, Indeok Hwang, Hyeonsook Cheong, Woo Sung Lee, Yong-sic Hwang, and Jun Lim*

Department of Bioscience and Biotechnology, Konkuk University, Seoul 143–701, Korea (S.A.L., E.K.Y., J.-O.H., M.-H.L., Y.-s.H., J.L.); Department of Biotechnology, Chosun University, Gwangju 501–759, Korea (I.H., H.C.); and Department of Biological Science, Sungkyunkwan University, Suwon 440–746, Korea (W.S.L.)

Sugars play important roles in many aspects of plant growth and development, acting as both energy sources and signaling molecules. With the successful use of genetic approaches, the molecular components involved in sugar signaling have been identified and their regulatory roles in the pathways have been elucidated. Here, we describe novel mutants of Arabidopsis (*Arabidopsis thaliana*), named *glucose insensitive growth* (*gig*), identified by their insensitivity to high-glucose (Glc)-induced growth inhibition. The *gig* mutant displayed retarded growth under normal growth conditions and also showed alterations in the expression of Glc-responsive genes under high-Glc conditions. Our molecular identification reveals that *GIG* encodes the plastidial copper (Cu) transporter PAA1 (for P_{1B}-type ATPase 1). Interestingly, double mutant analysis indicated that in high Glc, *gig* is epistatic to both *hexokinase1* (*hxk1*) and *aba insensitive4* (*abi4*), major regulators in sugar and retrograde signaling. Under high-Glc conditions, the addition of Cu had no effect on the recovery of *gig/paa1* to the wild type, whereas exogenous Cu feeding could suppress its phenotype under normal growth conditions. The expression of *GIG/PAA1* was also altered by mutations in the nuclear factors HXK1, ABI3, and ABI4 in high Glc. Furthermore, a transient expression assay revealed the interaction between ABI4 and the *GIG/PAA1* promoter, suggesting that ABI4 actively regulates the transcription of *GIG/PAA1*, likely binding to the CCAC/ACGT core element of the *GIG/PAA1* promoter. Our findings indicate that the plastidial Cu transporter PAA1, which is essential for plastid function and/or activity, plays an important role in bidirectional communication between the plastid and the nucleus in high Glc.

Sugars have multifaceted roles in plant growth and development, including their roles as energy sources and signaling molecules (Smeekens, 2000; Ramon et al., 2008). During the life cycle, plants can sense sugar levels, control the expression of many genes involved in physiological and developmental processes accordingly, and thus modulate growth and development to adapt to changes in sugar levels (Smeekens, 2000; Gibson, 2005; Rolland et al., 2006; Ramon et al., 2008). Genetic approaches have been fruitful in elucidating the molecular components in sugar signaling; several Arabidopsis (*Arabidopsis thaliana*) mutants insensitive to high-sugar conditions have been isolated and well characterized at the molecular level (Smeekens, 2000; Rook and Bevan, 2003; Gibson, 2005; Rolland et al., 2006; Ramon et al., 2008). In particular, *glucose insensitive* (*gin*) mutant seedlings are able to grow in the presence of 6% (w/v) Glc, which causes developmental arrest in wild-type seedlings (León and Sheen, 2003; Gibson, 2005). Some of these mutants are allelic to abscisic acid (ABA) biosynthesis (e.g. *gin1/aba2* and *gin5/aba3*) or signaling mutants (e.g. *gin6/aba insensitive4* [*abi4*]), demonstrating extensive interactions between sugar and phytohormone ABA (Arenas-Huertero et al., 2000; Cheng et al., 2002; Finkelstein and Gibson, 2002; León and Sheen, 2003; Gibson, 2005). In addition, the *GIN2* locus encodes a hexokinase (HXK1), which phosphorylates Glc to glucose-6-phosphate, and the *gin2* mutants overcome developmental arrest in the presence of 6% Glc (Moore et al., 2003). It has also been well established that HXK1 acts as an evolutionarily conserved Glc sensor in sugar signaling (Moore et al., 2003; Rolland et al., 2006). Coordination of growth and developmental responses to sugar levels is a complex process due to the existence of cross talk between sugar and other signaling pathways.

Plastids are known as sites of photosynthesis and of the synthesis and storage of biomolecules such as

[1] This work was supported by the Konkuk University Research Fund 2010.

* Corresponding author; e-mail jlim@konkuk.ac.kr.

The author responsible for distribution of materials integral to the findings presented in this article in accordance with the policy described in the Instructions for Authors (www.plantphysiol.org) is: Jun Lim (jlim@konkuk.ac.kr).

[W] The online version of this article contains Web-only data.

[OA] Open Access articles can be viewed online without a subscription.

www.plantphysiol.org/cgi/doi/10.1104/pp.111.191726

carbohydrates and hormones (Buchanan et al., 2000; Jung and Chory, 2010). Thus, the developmental, functional, and metabolic states of plastids can act as signals that modify the expression of nuclear genes (Nott et al., 2006; Pogson et al., 2008; Kleine et al., 2009; Pfannschmidt, 2010). Extensive genetic screens have been undertaken to identify mutants impaired in the plastid-to-nucleus retrograde signaling. Such mutants showed loss of intercompartmental communication, including aberrant control of the expression of nucleus-encoded plastid genes at the transcriptional level (Nott et al., 2006; Koussevitzky et al., 2007; Pogson et al., 2008). Interestingly, the ABA signaling pathway is also implicated in retrograde signaling (Penfield et al., 2006; Shen et al., 2006; Koussevitzky et al., 2007; Kim et al., 2009; Priest et al., 2009; Jung and Chory, 2010; Leister et al., 2011). Indeed, Koussevitzky et al. (2007) demonstrated that ABI4, an AP2-type transcription factor, serves as a point of convergence and regulates nuclear gene expression in retrograde signaling. However, the impact of sugars on interorganellar communication between the plastid and the nucleus is relatively unexplored.

Copper (Cu) is a microelement essential for living organisms as a cofactor (Palmer and Guerinot, 2009). However, excess Cu causes visible toxicity in Arabidopsis, indicating that adequate amounts need to be delivered to the various subcellular compartments (Shikanai et al., 2003; Abdel-Ghany et al., 2005; Palmer and Guerinot, 2009). In particular, the Arabidopsis plastidial P_{1B}-type ATPase Cu transporters, PAA1 (also known as AtHMA6) and its closest homolog PAA2 (also known as AtHMA8), play an important role in Cu delivery to plastids and, as a result, in the maintenance of Cu homeostasis (Shikanai et al., 2003; Abdel-Ghany et al., 2005). The Cu transporter PAA1, localized to the inner chloroplast envelope, transports Cu across the envelope into the stroma, and PAA2, localized to the thylakoid membrane, further transports Cu into the thylakoid lumen (Shikanai et al., 2003; Abdel-Ghany et al., 2005). Not surprisingly, *paa1 paa2* double mutants are seedling lethal, indicating their important roles in Cu delivery during postembryonic growth and development (Shikanai et al., 2003; Abdel-Ghany et al., 2005). However, the potential role of PAA1 in sugar-induced intercompartmental signaling is largely unknown.

In a screen for altered response in sugar signaling, we identified novel Arabidopsis mutants with insensitivity to growth inhibition in the presence of 6% Glc. We report here the genetic and physiological analyses of the recessive Glc-insensitive *gig* mutants (for *glucose insensitive growth*). In the presence of 1% Glc, however, the *gig* mutants showed a reduction of division potential in the root meristem, resulting in the retardation of root growth. Interestingly, under high-Glc conditions, *gig* is epistatic to both *hxk1* and *abi4*, and the expression levels of the nuclear genes, in particular *ABI4* and *HXK1*, were significantly decreased in *gig*. We found that the *GIG* locus encodes the plastidial P_{1B}-type ATPase Cu transporter PAA1 (Shikanai et al., 2003; Williams and Mills, 2005). Under high-Glc conditions, the addition of Cu had no effect on the recovery of *gig/paa1* to the wild type, whereas exogenous Cu feeding, as reported previously (Shikanai et al., 2003), could suppress its phenotype under normal growth conditions. In the presence of 6% Glc, the expression of *GIG/PAA1* was also altered by mutations in the nuclear factors HXK1, ABI3, and ABI4. A transient expression assay further revealed the interaction between ABI4 and the *GIG/PAA1* promoter, suggesting that ABI4 actively regulates the transcription of *GIG/PAA1*, likely binding to the CCAC/ACGT core element of the *GIG/PAA1* promoter. Our findings provide evidence for a novel function of the plastidial

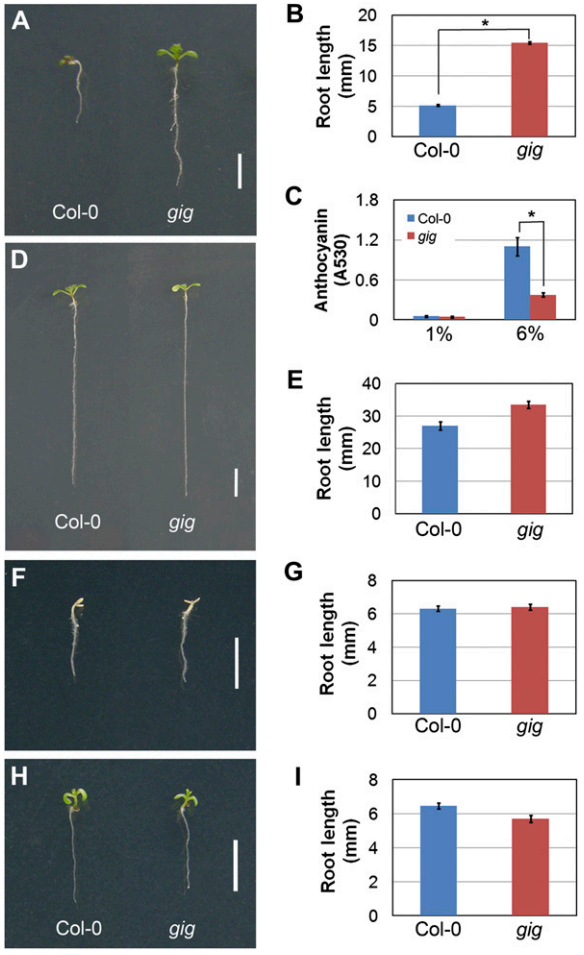

Figure 1. Isolation of *gig* with insensitivity to growth inhibition in the presence of 6% Glc. A, D, F, and H, Twelve-day-old seedlings of Col-0 (left) and *gig* (right) were grown on MS agar plates with different sugars as indicated: 6% Glc (A), 6% Suc (D), 12% Suc (F), and 300 mM mannitol (H). B, E, G, and I, Measurement of root length of 12-d-old seedlings in the presence of different sugars as indicated: 6% Glc (B), 6% Suc (E), 12% Suc (G), and 300 mM mannitol (I). C, Anthocyanin accumulation in Col-0 (blue) and *gig* (red) grown on 1% and 6% Glc. Statistical significance of differences was determined by Student's *t* test (* $P < 0.05$). Error bars indicate SE from three biological replicates. Bars = 0.5 cm.

Table I. *Genetic analysis of* gig *mutants*

Mutant	Phenotype		Total	Segregation Ratio	χ^2
	Sensitive	Insensitive			
Col-0 × *gig* F2	99	37	136	3:1	0.35 ($P \geq 0.05$)

PAA1 Cu transporter in bidirectional ("plastid-to-nucleus" and "nucleus-to-plastid") communication in response to high Glc levels.

RESULTS

Identification of Novel Mutants Insensitive to High-Glc-Induced Growth Inhibition

To date, genetic approaches have been successful in identifying constituents and elucidating their roles in sugar signaling (Smeekens, 2000; Rook and Bevan, 2003; Gibson, 2005; Rolland et al., 2006; Ramon et al., 2008). In an attempt to identify additional components in the sugar signaling pathway, we screened a population of approximately 1,500 M2 activation-tagged lines for insensitivity to growth arrest under high-Glc conditions. In the mutant screening, we identified one line that exhibited insensitivity to the inhibition of seedling growth in the presence of 6% Glc (Fig. 1A). In a root growth assay, root length of the line was longer, by approximately 3-fold, than that of wild-type Columbia (Col-0) seedlings (Fig. 1B). In addition, we analyzed anthocyanin accumulation, which is enhanced by high-Glc-induced growth inhibition (Tsukaya et al., 1991; Mita et al., 1997; Xiao et al., 2000; Baier et al., 2004; Teng et al., 2005; Jeong et al., 2010), in this mutant line. In the presence of 6% Glc, anthocyanin accumulation in the mutant was reduced by approximately 2.5-fold compared with that in Col-0 (Fig. 1C). Our findings indicate that the mutant line exhibits an insensitive growth phenotype in high (6%) Glc. To determine whether the insensitive growth phenotype is Glc specific, we analyzed this mutant line under high-Suc conditions. In the presence of 6% Suc, root growth of the mutant was slightly more insensitive than in the wild type (Fig. 1, D and E). When grown in the presence of 12% Suc, which is nearly the same as 6% Glc in molarity, the growth phenotype of the mutant line was almost indistinguishable from Col-0 seedlings (Fig. 1, F and G). To test whether the phenotype was attributable to osmotic stress, we cultured both Col-0 and the mutant in the presence of 300 mM mannitol, which is also the same as 6% Glc in molarity. We found that both the mutant and Col-0 seedlings were indistinguishably similar in growth (Fig. 1, H and I). Our observations indicate that the insensitive growth phenotype of the mutant was attributed primarily to high levels of exogenous Glc, and hence we named the mutant *gig*. For further genetic analysis, *gig* was backcrossed at least four times to Col-0 and could be reproducibly identified in the F2 progeny based on its insensitivity to 6% Glc. Under high-Glc conditions, *gig* was segregated in the typical 3:1 ratio, indicating that the *gig* mutation was inherited as a single recessive Mendelian locus (Table I).

The *gig* Mutant Exhibits Growth Retardation under Normal Growth Conditions

To address whether its insensitive growth phenotype in the presence of 6% Glc is due to relatively

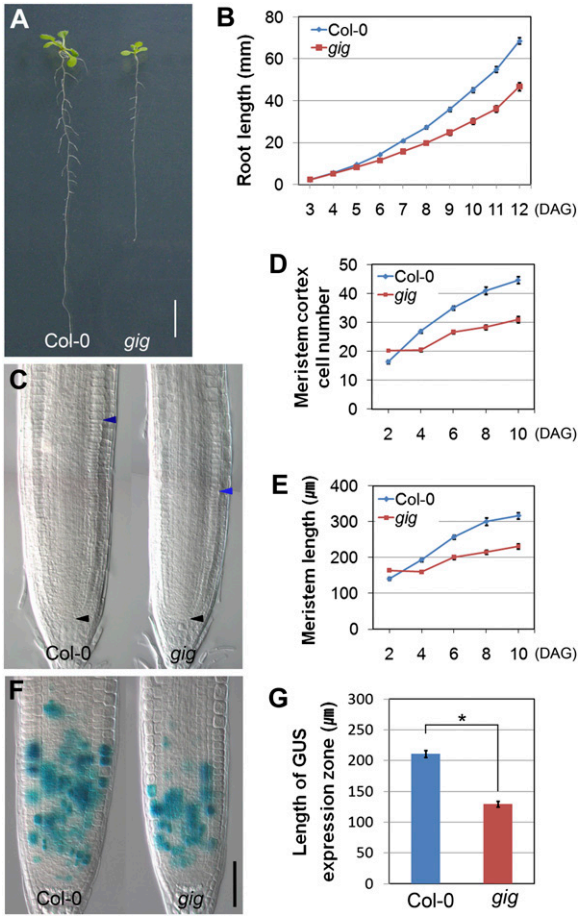

Figure 2. Growth retardation of *gig* under normal conditions. A, Twelve-day-old seedlings of Col-0 (left) and *gig* (right) grown on MS agar plates with 1% Glc. Bar = 1 cm. B, Root growth assay of Col-0 and *gig* seedlings from 3 to 12 d after germination (DAG). C, Differential interference contrast image of root meristem size of Col-0 and *gig* at 8 DAG. Black arrowheads indicate the QC, whereas blue arrowheads demarcate the upper margin of the MZ. D and E, Measurement of meristem cortex cell number (D) and meristem length (E) from 2 to 10 DAG. F, *CYCB1*::*GUS* expression in Col-0 and *gig* roots at 7 DAG. Bar = 50 μm. G, Length of the *CYCB1*::*GUS* expression zone. Error bars indicate SE; * $P < 0.05$.

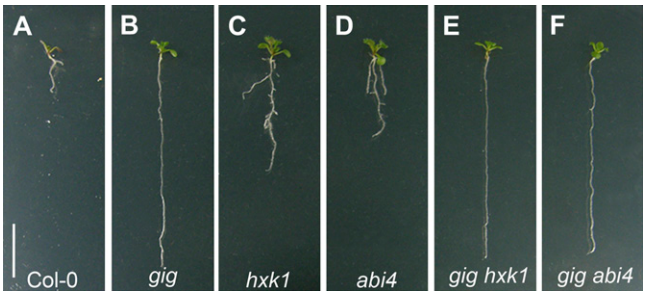

Figure 3. Genetic analysis of *gig hxk1* and *gig abi4* double mutants. Twelve-day-old seedlings of Col-0 (A), *gig* (B), *hxk1* (C), *abi4* (D), *gig hxk1* (E), and *gig abi4* (F) were grown on MS agar plates with 6% Glc. *gig* is epistatic to both *hxk1* and *abi4*. Bar = 1 cm.

lower inhibition of vigor in *gig* seedlings, we investigated the *gig* mutant in the presence of 1% Glc (hereafter referred to as normal growth conditions in this study). Interestingly, *gig* showed a short-root phenotype compared with Col-0 seedlings under normal growth conditions (Fig. 2A). In a root growth assay, we found that differences in the growth rate between Col-0 and *gig* increased gradually as plants became mature, indicating that *gig* root growth was retarded (Fig. 2B). We further investigated the root meristem size of *gig* by measuring the number and length of ground cells from the quiescent center (QC) in the presence of 1% Glc, as described previously (Dello Ioio et al., 2007; Achard et al., 2009; Ubeda-Tomás et al., 2009; Heo et al., 2011). The root meristem size of *gig* was smaller than that of Col-0, suggesting a reduction of cell division in the meristem zone (MZ; Fig. 2, C–E). To further characterize this defect, a CYCB1::GUS mitotic marker (Donnelly et al., 1999) was monitored both in *gig* and Col-0, and indeed cell division potential in *gig* roots was significantly reduced (Fig. 2, F and G). Our findings indicate that the retarded root growth of *gig* is attributable to a decrease in cell division potential. In the Arabidopsis root meristem, the stem cell niche, including the QC and initials, replenishes all the cell files (Scheres, 2007). We thus investigated developmental defects in and around the stem cell niche of *gig* using cell-specific markers, including SCARECROW (SCR), SHORT-ROOT (SHR), QC25, and WUSCHEL RELATED HOMEOBOX5 (WOX5; Di Laurenzio et al., 1996; Helariutta et al., 2000; Nakajima et al., 2001; Sabatini et al., 2003; Gallagher et al., 2004; Sarkar et al., 2007). In the presence of 1% Glc, the stem cell niche of *gig* was indistinguishable from that of Col-0, indicating that the reduction of the root meristem size of *gig* is not due to defects in the stem cell niche (Supplemental Fig. S1). In addition to its short-root phenotype, *gig* adult plants were also dwarf compared with Col-0 under our growth conditions (16-h-light/8-h-dark cycles; Supplemental Fig. S2). Taken together, *gig* exhibited growth retardation under normal (1% Glc) growth conditions, unlike its insensitive growth under high-Glc (6% Glc) conditions.

The *gig* Mutant Is Epistatic to *abi4* and *hxk1* under High-Glc Conditions

The insensitive phenotype under high-Glc conditions raised the question of whether *GIG* plays a role in sugar signaling. To address this question, we adopted a genetic approach by using *hxk1/gin2* and *abi4/gin6* mutants, which are well-characterized mutants with defects in sugar signaling (Arenas-Huertero et al., 2000; Huijser et al., 2000; Finkelstein and Gibson, 2002; Arroyo et al., 2003; Moore et al., 2003; Acevedo-Hernández et al., 2005; Dekkers et al., 2008). In the presence of 6% Glc, both *hxk1* and *abi4*, as expected, exhibited insensitivity to growth arrest compared with Col-0 seedlings (Fig. 3, A, C, and D). Intriguingly, *gig* was more insensitive in root growth compared with both *hxk1* and *abi4* under high-Glc conditions (Fig. 3, B–D). To investigate genetic interactions of *gig* and these mutants, we generated the double mutant combinations of *gig hxk1* and *gig abi4*, respectively, and examined the growth phenotype in the presence of 6% Glc. To our surprise, the seedling growth of both *gig hxk1* and *gig abi4* was indistinguishable from that of the *gig* single mutant (Fig. 3, B, E, and F). Our findings

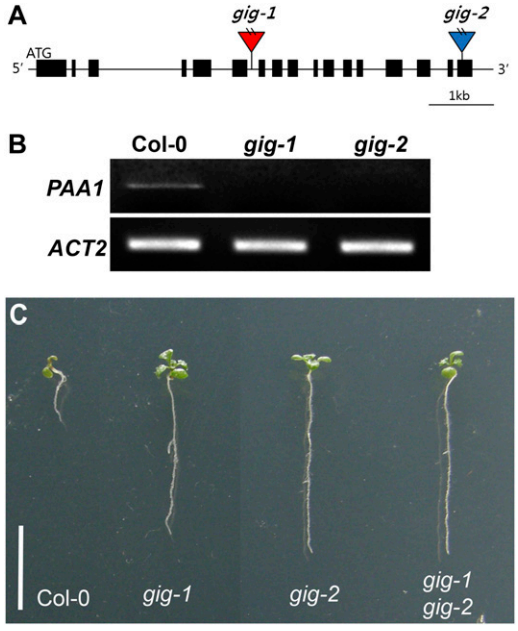

Figure 4. Molecular identification of the *GIG* locus. A, Location of T-DNA insertions. The boxes depict the coding regions, whereas the lines represent the noncoding regions. The red triangle denotes the position of a T-DNA insertion in *gig-1* that is isolated from an activation-tagged population, whereas the blue triangle indicates the T-DNA insertion site in *gig-2* that was identified from the SALK T-DNA database. The *GIG* locus encodes the plastidial P_{1B}-type ATPase Cu transporter PAA1. B, Expression of *PAA1* in Col-0, *gig-1*, and *gig-2* seedlings. No expression was detected in either *gig-1* or *gig-2* seedlings. C, Allelism test of *gig-1* and *gig-2*. From left to right, Col-0, *gig-1*, *gig-2*, and F1 progeny of a cross between *gig-1* and *gig-2* (*gig-1 gig-2*). The F1 progeny show insensitivity to growth inhibition in 6% Glc. Bar = 1 cm.

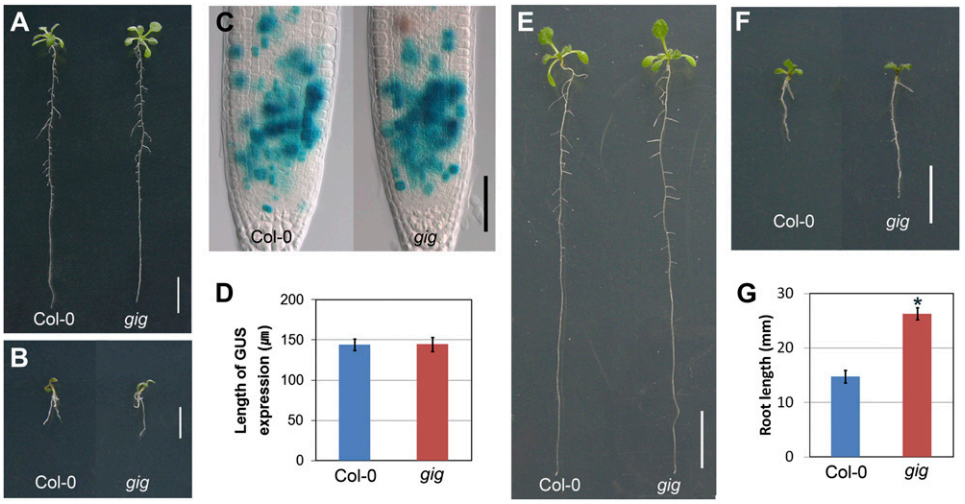

Figure 5. Complementation of *gig/paa1* mutants. A and B, The genomic fragment, encompassing the predicted promoter and ORF, fused to GFP (*pGIG*::*GIG-GFP*) restores defects in *gig* in the presence of 1% (A) and 6% (B) Glc. C and D, Restoration of defects in *gig* with Cu supplement. Shown are a differential interference contrast image of *CYCB1*::*GUS* expression (C) and the length of the *CYCB1*::*GUS* expression zone (D) of Col-0 and *gig* in the presence of 10 μM $CuSO_4$. Bar = 50 μm. E to G, Twelve-day-old seedlings of Col-0 (left) and *gig* (right) grown on 1% (E) and 6% (F and G) Glc MS agar plates supplemented with 10 μM $CuSO_4$. Bars = 1 cm in A, B, E, and F.

indicate that *gig* is epistatic to both *hxk1* and *abi4* in high Glc.

GIG Encodes the Plastidial P_{1B}-Type ATPase Cu Transporter PAA1

To determine the molecular basis of the *gig* phenotypes, we identified the *GIG* locus using thermal asymmetric interlaced PCR (Liu et al., 1995), since the mutant was initially isolated in an activation-tagged population. We found a T-DNA insertion in the sixth intron of the *GIG* locus (At4g33520; Fig. 4A), which encodes the plastidial P_{1B}-type ATPase Cu transporter PAA1 (also known as AtHMA6; Shikanai et al., 2003; Williams and Mills, 2005). Previous studies have demonstrated that PAA1, localized in the chloroplast inner membrane, mediates Cu delivery into the stroma (Shikanai et al., 2003; Abdel-Ghany et al., 2005). With specific primers for *PAA1*, we detected no expression, indicating that, in accordance with our genetic analysis, *gig* is a loss-of-function mutant (Fig. 4B; Table I). Additionally, we identified another T-DNA insertion allele in the SALK database (http://signal.salk.edu) and found that this new allele, named *gig-2* (SALK_043208; Fig. 4, A and B), was also similarly insensitive to growth inhibition under high-Glc conditions (Fig. 4C). Subsequently, we reciprocally crossed these mutants for a complementation test. In the presence of 6% Glc, the F1 progeny of *gig-1* and *gig-2* showed indistinguishably insensitive growth compared with each parental line (Fig. 4C), corroborating their allelic relation. To further verify whether mutations in the *GIG/PAA1* locus cause the growth insensitivity to high levels of exogenous Glc, we transformed *gig* mutants with a translational fusion (hereafter referred to as *pGIG*::*GIG-GFP*), including 443 bp of the putative promoter region and the open reading frame (ORF) fused to GFP. In the presence of 1% Glc, the translational fusion restored the retarded *gig* growth phenotype to Col-0 (Fig. 5A). As expected, transgenic seedlings with *pGIG*::*GIG-GFP* exhibited similar sensitivity to high-Glc-induced growth inhibition compared with Col-0 (Fig. 5B). Taken together, our findings indicate that the insensitivity of *gig* to high-Glc-induced growth inhibition is, indeed, due to the loss of the plastidial Cu transporter PAA1 function.

The *gig/paa1* Mutant Is Not Rescued by Cu Addition In High Glc

Previously, it was shown that *paa1* mutants had a lower Cu content in the chloroplast and that the addition of exogenous 10 μM $CuSO_4$ could suppress growth defects, indicating that PAA1, which mediates Cu delivery across the plastid envelope, is an essential component of the plastidial Cu transport system (Shikanai et al., 2003). Hence, we cultured *gig/paa1* on Murashige and Skoog (MS) agar plates with increasing Cu concentrations (5, 10, and 50 μM). When grown on MS agar plates supplemented with 10 μM $CuSO_4$, the growth of *gig* in the presence of 1% Glc was nearly indistinguishable from Col-0 seedlings (Fig. 5, C–E; Supplemental Fig. S3). As Shikanai et al. (2003) demonstrated previously, in the presence of 50 μM $CuSO_4$, the growth of both Col-0 and *gig/paa1* roots was inhibited (data not shown), indicating that the addition of high (50 μM) $CuSO_4$ adversely affected seedling development of both Col-0 and *gig/paa1*. To further

assess the relationship between Cu and Glc, we analyzed the root growth of Col-0 and *gig/paa1* in the absence or presence of 10 μM $CuSO_4$ with increasing Glc concentrations. In the absence of 10 μM $CuSO_4$, the growth of *gig/paa1* was retarded, as expected, compared with Col-0, up to the point where exogenous Glc was added to 3% (w/v; Supplemental Fig. S4A). Whereas both Col-0 and *gig/paa1* were nearly identical in the presence of 4% Glc, the difference in growth between Col-0 and *gig/paa1* became reversed under high-Glc conditions, in that *gig/paa1* was more insensitive. When supplemented with 10 μM $CuSO_4$, however, *gig/paa1* was nearly indistinguishable from Col-0 seedlings up to 5% Glc (Supplemental Fig. S4B). Interestingly, *gig/paa1* was still insensitive to high (6% and 7%) Glc, with no recovery of the growth defect (Fig. 5, F and G; Supplemental Fig. S4B). These findings indicate that the addition of Cu had no effect on reverting *gig/paa1* to the wild type under high-Glc conditions, whereas exogenous Cu feeding could suppress its phenotype under normal growth conditions.

Expression Analysis of *GIG/PAA1*

To obtain further insight into *gig/paa1* phenotypes, we investigated the in planta expression patterns of *GIG/PAA1*. To this end, we generated transgenic lines harboring a transcriptional fusion of the GUS marker gene under the control of the *GIG/PAA1* cis-regulatory sequence located upstream of the ORF (hereafter referred to as *pGIG*::*GUS*). The putative promoter sequence selected was the longest that was used for molecular complementation of the *gig/paa1* mutant. Therefore, we expected that this cis-regulatory sequence would be informative in monitoring the expression patterns of *GIG/PAA1* in planta. In the shoot of 12-d-old seedlings, we observed GUS staining in marginal regions of cotyledons and leaves and primarily in the vasculature (Fig. 6, A and B). In the root, the *GIG/PAA1* expression was rather cell type specific, being detected only in the vascular tissues (Fig. 6C). In parallel, we also analyzed the seedling root with *pGIG*::*GIG-GFP* (translational fusion), and similarly, localization of GIG-GFP was observed only in the vasculature (Fig. 6D). For a more detailed analysis, we generated transverse sections of the primary root and detected GUS expression in the vascular bundle (Fig. 6E). Interestingly, however, no GUS expression was detected in the root tip (Fig. 6F), implying that cells in the MZ are more sensitive to fluctuations in Glc levels. Our findings suggest the involvement of the plastidial Cu transporter PAA1 in nongreen tissues, in which we primarily observed the growth retardation in *gig*. We also analyzed the levels of *GIG/PAA1* expression by an independent, complementary method: reverse transcription-based quantitative (qRT)-PCR. In our analysis, the expression of *GIG/PAA1* was detected in various organs, with the highest expression in the flower (Fig. 6G). Additionally, the levels of *GIG/PAA1* mRNA accumulation were significantly increased, by approximately 3-fold, in the presence of 6% Glc, indicating that its expression is also subject to regulation by high Glc (Fig. 6H).

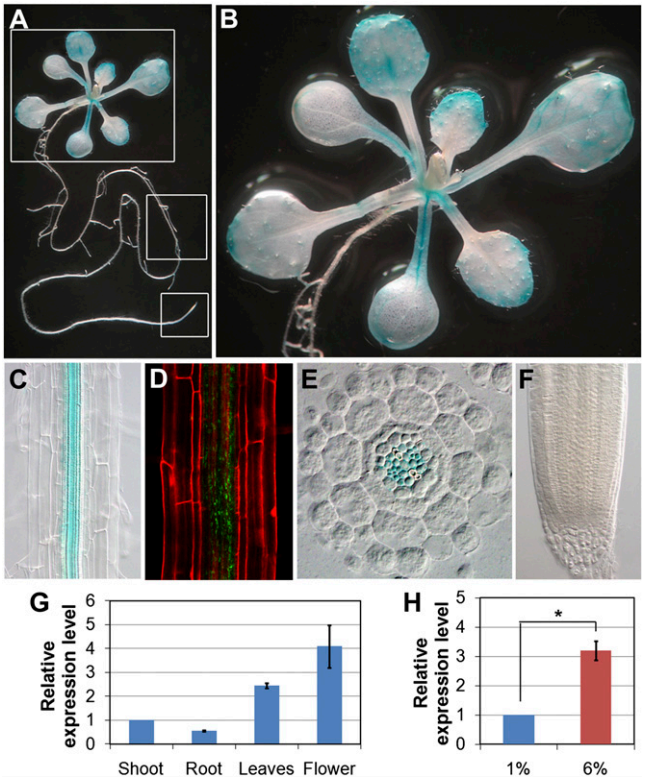

Figure 6. Expression pattern of *GIG/PAA1*. A to C, Tissue-specific expression of the transcriptional GUS fusion (*pGIG*::*GUS*) in the whole seedling (A), shoot (B), and root (C). D, Confocal image of the translational GFP fusion (*pGIG*::*GIG-GFP*) in the root. E, Transverse root section of 12-d-old seedling. Blue GUS staining is detected only in the vasculature. F, No expression is detectable in the root tip. G, *GIG* transcript levels in different organs as determined by qRT-PCR. The *GIG* mRNA level in the shoot is arbitrarily set to 1. H, Expression of *GIG* in the presence of 1% and 6% Glc by qRT-PCR. The statistical significance of differences was determined by Student's *t* test (* $P < 0.05$). Error bars indicate SE from three biological replicates.

Expression of Glc-Responsive Genes in *gig/paa1*

In addition to growth arrest, high levels of exogenous Glc also regulate a wide variety of genes at the transcriptional level, including *APL3* (a large subunit of ADP-Glc pyrophosphorylase involved in starch biosynthesis) and *CHS* (for chalcone synthase; Koch, 1996; Li et al., 2006). Hence, we analyzed the expression levels of these Glc-responsive genes in both Col-0 and *gig/paa1* in the presence of 1% and 6% Glc. Under high-Glc conditions, the *APL3* mRNA level was, as expected, markedly elevated in Col-0, whereas the level of induction was significantly reduced in *gig/paa1* (Fig. 7A). Likewise, the *CHS* mRNA level was increased in the presence of 6% Glc, but in *gig/paa1*, the level of induction was significantly reduced (Fig. 7B). On the basis of our findings that *gig* is epistatic to both

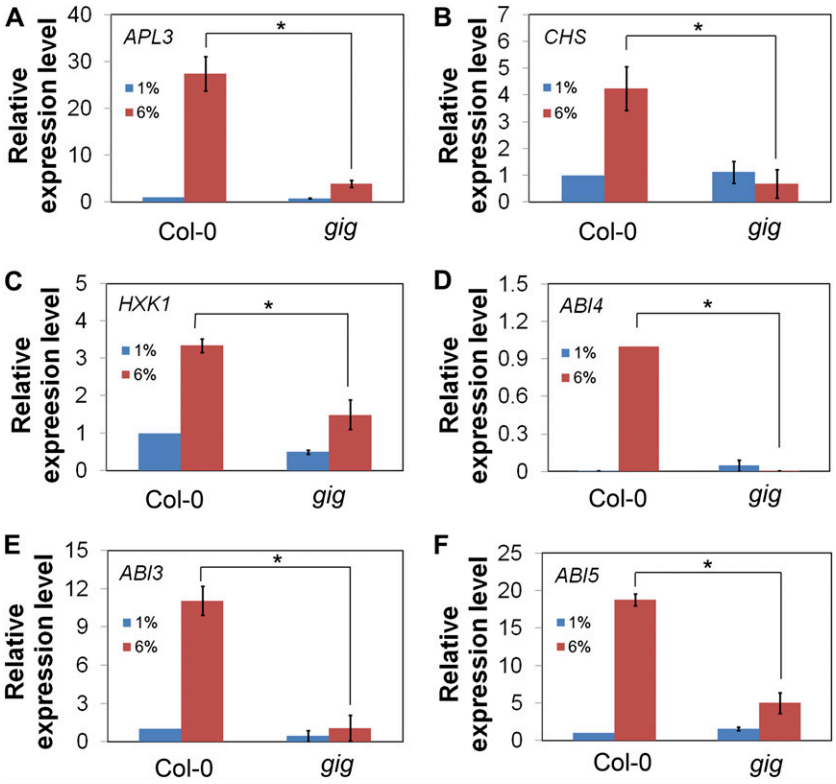

Figure 7. Expression analysis of Glc-responsive genes. qRT-PCR in Col-0 and *gig* is shown in the presence of 1% (blue) and 6% (red) Glc. A, *APL3*. B, *CHS*. C, *HXK1*. D, *ABI4*. E, *ABI3*. F, *ABI5*. The statistical significance of differences was determined by Student's *t* test (* $P < 0.05$). Error bars indicate SE from biological triplicates.

abi4 and *hxk1* in response to high-Glc concentrations, we subsequently analyzed the transcript levels of *ABI4* and *HXK1* in Col-0 and *gig/paa1* in the presence of 1% and 6% Glc. Under high-Glc concentrations, the *HXK1* mRNA level was, as expected, also induced by approximately 3-fold in Col-0, whereas it was significantly reduced in *gig/paa1* (Fig. 7C). Interestingly, high-Glc activation of *ABI4* was completely abolished in *gig/paa1* (Fig. 7D). To investigate the extent of Glc-induced gene regulation, we also examined the *ABI3* and *ABI5* expression levels, which are known to be induced by high Glc (Cheng et al., 2002; Arroyo et al., 2003; Yuan and Wysocka-Diller, 2006; Dekkers et al., 2008). In the presence of 6% Glc, such Glc activation of *ABI3* was almost completely eliminated in *gig/paa1* (Fig. 7E). Likewise, induction of *ABI5* expression was markedly reduced in *gig/paa1* (Fig. 7F). Furthermore, we also analyzed the expression of *APL3*, *HXK1*, and *ABI4* in the presence of 10 μM $CuSO_4$. Interestingly, the expression levels of these genes in *gig/paa1* were not

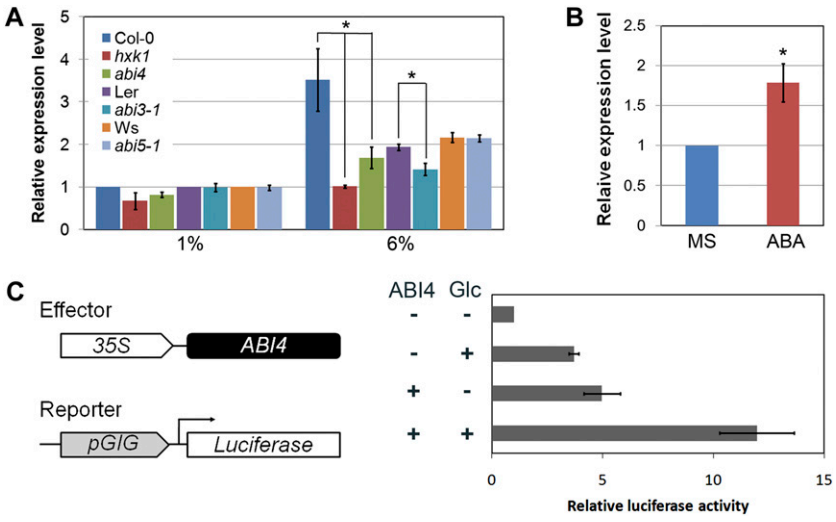

Figure 8. Regulation of *GIG* expression levels by ABA. A, *GIG* transcript levels in *abi3*, *abi4*, *abi5*, and *hxk1* in the presence of 1% and 6% Glc. B, Expression of *GIG* in the absence or presence of 10 μM ABA. C, Transient expression assay for the interaction between ABI4 and the *GIG* promoter. The effector and reporter plasmids are schematically shown. Relative LUC activity was determined by the addition of Glc alone, ABI4 alone, and both Glc and ABI4. Error bars indicate SE from biological triplicates.

recovered to the Col-0 levels (Supplemental Fig. S5). This observation is consistent with our previous finding (Fig. 5, F and G; Supplemental Fig. S4) that the addition of Cu in high Glc could not suppress the *gig/paa1* phenotype.

Taken together, our expression studies indicate that the loss of the plastidial Cu transporter PAA1 function significantly alters the expression levels of Glc-responsive genes. In particular, a reduction of the expression of nuclear factors ABI3, ABI4, ABI5, and HXK1 in *gig/paa1* under high-Glc conditions suggests a novel retrograde plastid-to-nucleus signaling, in which the plastidial Cu transporter PAA1 is involved.

ABI4 Is Essential for the Activation of *GIG/PAA1* Expression

Our findings that the loss of GIG/PAA1 function results in a dramatic reduction of the nuclear gene expression of *ABI3*, *ABI4*, *ABI5*, and *HXK1* in the presence of high Glc and that the *GIG/PAA1* promoter itself contains a CCAC/ACGT sequence for ABI4 binding (Supplemental Fig. S6; Strand et al., 2003; Koussevitzky et al., 2007) raised the question of whether the transcription of *GIG/PAA1* itself is subject to regulation by the nuclear transcription factor ABI4. To test this, we first examined the expression of *GIG/PAA1* in *abi3*, *abi4*, and *abi5* in the presence of 1% and 6% Glc. As shown in Figure 8A, the *GIG/PAA1* mRNA levels were significantly reduced in both *abi3* and *abi4*, but not in *abi5*, under high-Glc conditions. In addition, we also monitored the *GIG/PAA1* expression in *hxk1* in the presence of 1% and 6% Glc, since the Glc sensor HXK1 can be localized in the nucleus and regulate gene expression (Cho et al., 2006). In high Glc, the induction of *GIG/PAA1* mRNA was almost completely abolished in *hxk1* (Fig. 8A). Next, we addressed whether the expression of *GIG/PAA1* is regulated by ABA. Indeed, the level of *GIG/PAA1* mRNA accumulation was substantially increased in the presence of 10 μM ABA (Fig. 8B).

To further investigate the interaction between ABI4 and the *GIG/PAA1* promoter, we performed a transient expression assay using Arabidopsis protoplasts as described previously (Yoo et al., 2007). The reporter plasmid containing the 443-bp fragment that was used for both transcriptional fusion and molecular complementation, and the effector plasmid 35S::ABI4, were introduced into Arabidopsis protoplasts in the absence or presence of high Glc (300 mM). When relative luciferase (LUC) activity was monitored, the expression of *GIG/PAA1* was, as expected, induced by high Glc alone and ABI4 alone (Fig. 8C). Interestingly, *GIG/PAA1* expression was synergistically induced by both high Glc and ABI4, suggesting that the nuclear transcription factor ABI4 actively regulates the transcription of *GIG/PAA1* that is essential for plastid function and/or activity. Our findings suggest a molecular mechanism of bidirectional (plastid-to-nucleus and nucleus-to-plastid) communication in response to high Glc levels.

DISCUSSION

In this study, we identified novel mutants, designated *gig*, that showed insensitivity to growth inhibition in high (6%) Glc. The expression levels of Glc-responsive *ABI3*, *ABI4*, *ABI5*, *APL3*, *CHS*, and *HXK1* genes were significantly altered in *gig/paa1* in the presence of 6% Glc. Interestingly, *gig abi4* and *gig hxk1* double mutants were indistinguishable from the *gig* single mutant under high-Glc conditions, indicating that *gig* is epistatic to both *abi4* and *hxk1*. Subsequent molecular cloning led us to the conclusion that the insensitivity to high-Glc-induced growth inhibition was caused by the loss of plastidial Cu transporter PAA1 function (Shikanai et al., 2003). When complemented with the *GIG/PAA1* genomic fragment or supplemented with exogenous Cu, growth defects in the *gig/paa1* mutants were completely restored to levels indistinguishable from Col-0 seedlings. These results, together with those from the phenotypic analyses of *gig/paa1*, indicate the important role of the GIG/PAA1 Cu transporter in Glc-induced retrograde plastid-to-nucleus signaling. In retrograde signaling, particularly plastid signaling revealed in this study, integrated information on developmental, functional, and metabolic states is conveyed to the nucleus, in which the expression of nuclear genes is modified accordingly (Nott et al., 2006; Pogson et al., 2008; Kleine et al., 2009; Pfannschmidt, 2010; Leister et al., 2011). In particular, ABI4 plays an important role in the integration of retrograde signaling to regulate the transcription of nuclear genes (Koussevitzky et al., 2007). Furthermore, intracellular communication between the plastid and the nucleus, as

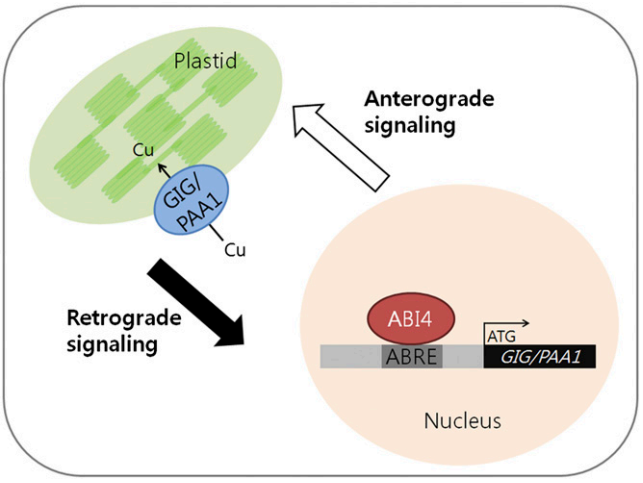

Figure 9. Bidirectional communication between the chloroplast and the nucleus. Changes in the functional states/activities of plastids caused by high Glc can possibly act as a retrograde signal to alter the expression of nuclear genes such as *ABI3*, *ABI4*, *ABI5*, and *HXK1*. In particular, the transcription factor ABI4, which likely binds directly to the CCAC/ACGT core element of the *GIG/PAA1* promoter, regulates the expression of the plastidial Cu transporter PAA1 that is essential for plastid function and/or activity.

suggested previously (Jung and Chory, 2010), is essentially bidirectional. Thus, we investigated whether the *GIG/PAA1* gene itself is subject to transcriptional regulation by the nuclear transcription factor ABI4. First, we found a significant reduction of the *GIG/PAA1* transcript levels in *abi3*, *abi4*, and *hxk1* mutants. Next, we analyzed the interaction between ABI4 and the *GIG/PAA1* promoter, which contains a combination of the CCAC/ACGT core element for ABI4 binding and retrograde signaling (Strand et al., 2003; Koussevitzky et al., 2007). Indeed, our transient expression assay reveals that the transcription of *GIG/PAA1* is synergistically regulated by high Glc and ABI4. These results lend support to our hypothesis that the plastidial Cu transporter PAA1 plays a role in the coordination of the bidirectional intercompartmental communication between the plastid and the nucleus in the presence of high Glc.

Previously, it was shown that miRNA398 levels, which function to repress two Cu/zinc superoxide dismutases (CSD1 and CSD2), were decreased by the addition of Cu (Sunkar et al., 2006; Yamasaki et al., 2007; Dugas and Bartel, 2008). Moreover, Dugas and Bartel (2008) demonstrated that in the presence of Suc, miRNA398 levels were increased, whereas the protein levels of CSD1 and CSD2, the miRNA398 targets, were substantially decreased. The inverse relationship between Cu and sugars in the regulation of miRNA398 levels, and in turn the CSD1 and CSD2 levels, suggests that sugars affect the results of Cu feeding. Interestingly, we also found that the addition of Cu could not revert *gig/paa1* to the wild type in the presence of high Glc. Since it was demonstrated that both transcript and protein levels of CSD1 and CSD2 were higher in *gig/paa1* than in the wild type (Shikanai et al., 2003; Abdel-Ghany et al., 2005), it will be interesting to determine the levels of miRNA398 accumulation in *gig/paa1* in the absence or presence of high Glc with the addition of Cu.

Since *GIG/PAA1* is expressed in roots as well as in green tissues (Shikanai et al., 2003; Abdel-Ghany et al., 2005) and reactive oxygen species (ROS) can modulate the balance between cell proliferation and differentiation in roots (Tsukagoshi et al., 2010), it is tempting to speculate that ROS and/or sugar levels in plastids of both roots and green tissues may be influenced by proper Cu delivery to CSD1 and CSD2, which is controlled by PAA1 (Shikanai et al., 2003; Abdel-Ghany et al., 2005). Thus, changes in ROS, sugar levels, functional states, and/or activities of plastids caused by high Glc can act as retrograde signals (Oswald et al., 2001; Fey et al., 2005) and in turn regulate the expression of nuclear genes such as *ABI3*, *ABI4*, *ABI5*, and *HXK1* (Nott et al., 2006; Koussevitzky et al., 2007; Pogson et al., 2008; Kleine et al., 2009; Pfannschmidt, 2010). Subsequently, alterations in the expression levels of the nuclear factors, in particular ABI4, which can bind directly to the CCAC/ACGT core element of the *GIG/PAA1* promoter, regulate the expression of the plastidial Cu transporter PAA1 that is essential for plastid function and/or activity (Fig. 9).

In summary, we report a previously unrecognized role for the plastidial Cu transporter PAA1 in the coordination of Glc-induced intracellular signaling. Further molecular and biochemical characterization with respect to the nature of retrograde signals (e.g. ROS, sugar levels, or both), for which GIG/PAA1 may well be responsible, will be necessary to elucidate the precise molecular mechanism of Glc-induced intercompartmental signaling between the plastid and the nucleus.

MATERIALS AND METHODS

Plant Materials and Growth Conditions

The Arabidopsis (*Arabidopsis thaliana*) ecotype Col-0 was used as the wild-type control in this study, except for *abi3-1* (Landsberg *erecta*) and *abi5-1* (Wassilewskija). The Col-0 T-DNA insertion mutants *hxk1* (SALK_070739) and *gig-2* (SALK_043208) were identified in the SIGnAL Web site (http://signal.salk.edu) and obtained from the Arabidopsis Biological Resource Center. Other mutant and transgenic lines used in this study have been described previously: *abi4-1* (Finkelstein et al., 1998), *CYCB1*::*GUS* (Donnelly et al., 1999), QC25 (Sabatini et al., 2003), *WOX5* (Sarkar et al., 2007), *SCR* (Di Laurenzio et al., 1996; Gallagher et al., 2004), and *SHR* (Helariutta et al., 2000; Nakajima et al., 2001). Seeds were sterilized with 2% sodium hypochlorite and 0.15% Tween 20 for 2 min and rinsed three to five times in sterile water. After stratification for 4 d in the dark at 4°C, seeds were cultured vertically on one-half-strength MS agar plates containing 1% (w/v) Glc, 6% (w/v; approximately 300 mM) Glc, 6% and 12% (approximately 350 mM) Suc, 300 mM (approximately 5.5%) mannitol, or 10 μM $CuSO_4$ as indicated (in culture rooms with a 16-h-light/8-h-dark cycle at 22°C). For adult plants, MS agar plate-grown seedlings were transferred to soil and grown to full maturity in culture rooms with a 16-h-light/8-h-dark cycle at 22°C as described previously (Heo et al., 2011).

Screening for *gig* and Isolation of the *GIG* Locus

For the identification of *gig*, an activation tagging library was generated as described (Weigel et al., 2000; Hwang et al., 2010). A population of approximately 1,500 M2 lines was screened for insensitivity to growth arrest on one-half-strength MS agar plates containing 6% (w/v) Glc. The *gig* mutant with enhanced high-Glc tolerance relative to wild-type seedlings was visually identified and was subsequently backcrossed to Col-0 at least four times for further analysis. To identify the *GIG* locus, thermal asymmetric interlaced PCR was performed as described previously (Liu et al., 1995). The primer sequences are listed in Supplemental Table S1.

Root Growth Assays and Statistical Analysis

Digital images of seedlings grown vertically on one-half-strength MS agar plates were taken using an SP-560UZ digital camera (Olympus) at each time point as indicated. Root length was measured from the digital images of the plates using ImageJ software (http://rsbweb.nih.gov/ij). The experiments were independently repeated three times, and the data were analyzed using the Excel statistical package (Microsoft). Student's *t* test was performed to compare the mean values of triplicates, and SE values are indicated.

Anthocyanin Quantitation

Anthocyanin accumulation in Arabidopsis seedlings was quantitatively determined as described previously (Mita et al., 1997; Teng et al., 2005; Solfanelli et al., 2006) with minor modifications. For anthocyanin extraction, frozen, homogenized seedlings (100 mg) at 12 d after germination were incubated with 800 μL of 1% (v/v) hydrochloric acid in methanol overnight at 4°C. Subsequently, 400 μL of distilled water and 200 μL of chloroform were added to the mixture and mixed vigorously by vortexing. After centrifugation at 13,000 rpm for 15 min, the supernatant was separated and the absorbance was measured at 530 and 657 nm using a spectrophotometer, as described previously (Mita et al., 1997; Teng et al., 2005; Solfanelli et al., 2006).

qRT-PCR Analysis

Total RNA samples were prepared from 12-d-old seedlings grown on one-half-strength MS agar plates, containing either 1% or 6% Glc, using Easy-Blue reagent (Intron). RNA samples were treated with RQ1 RNase free-DNase (Promega) to eliminate potential contamination of genomic DNA and further purified using an RNeasy Plant Mini kit according to the manufacturer's instructions (Qiagen). The quality and quantity of the isolated RNA were assessed by both gel electrophoresis and spectrophotometry as described previously (Lee et al., 2008; Heo et al., 2011). The protocols used for qRT-PCR were essentially the same as those described previously (Lee et al., 2008; Heo et al., 2011) with minor modifications. Approximately 0.5 μg of total RNA was used for the synthesis of cDNA using the iScript cDNA synthesis kit according to the manufacturer's instructions (Bio-Rad). These cDNA samples were used for qRT-PCR using SYBR Premix ExTaq reagents (Takara) with the Mx3000P QPCR System (Agilent Technologies). The *ACTIN2* (At3g18780) gene was used as the internal reference as described previously (Lee et al., 2008). Each experiment was conducted independently at least three times with biological replicates.

Plasmid Construction and Transformation

To generate a transcriptional fusion of the *GIG/PAA1* locus to the GUS reporter gene, a 443-bp fragment containing the cis-sequence upstream of the start codon, which is the longest intergenic region of the *GIG/PAA1* locus, was PCR amplified and subsequently cloned into the pENTR/D-TOPO vector (Invitrogen). The error-free promoter fragment of *GIG/PAA1* was subcloned into the binary pMDC162 vector (Curtis and Grossniklaus, 2003) by Gateway recombination cloning technology (Invitrogen).

For molecular complementation, we generated a translational fusion of the wild-type *GIG/PAA1* ORF to GFP under the control of the 443-bp *GIG/PAA1* promoter into the binary pMDC107 vector (Curtis and Grossniklaus, 2003) using Gateway technology (Invitrogen). The resulting plasmids were introduced into *Agrobacterium tumefaciens* (GV3101) and then introduced into Col-0 and *gig* plants by the floral dipping method (Clough and Bent, 1998).

For the transient expression assay, the reporter and effector plasmids were constructed using the pBI221 vector. In the reporter plasmid, the GUS gene was replaced with the firefly LUC gene, and the cauliflower mosaic virus 35S promoter was replaced with the 443-bp *GIG/PAA1* promoter. To generate the effector plasmid, the full-length ABI4 coding region was amplified by PCR and then inserted into pBI221, replacing the GUS gene. As a control plasmid, the GUS gene in pBI221 was replaced with the *Renilla* LUC gene.

Histochemical GUS Assays and Microscopy

The protocols used for the histochemical localization of GUS activity were essentially the same as those described previously (Yu et al., 2010; Heo et al., 2011) with minor modifications. MS agar plate-grown seedlings at 12 d after germination were incubated overnight at 37°C in GUS staining solution [0.4 mM 5-bromo-4-chloro-3-indoxyl-β-D-glucuronic acid, 2 mM $K_3Fe(CN)_6$, 2 mM $K_4Fe(CN)_6$, 0.1 M sodium phosphate, 10 mM EDTA, and 0.1% Triton X-100]. After staining overnight, the samples were washed and cleared as described (Yu et al., 2010; Heo et al., 2011). Plastic sections of GUS-stained roots were embedded in Technovit 7100 (Heraeus Kulzer) and sectioned using an HM 355S microtome (Microm) according to the previous instructions (Yu et al., 2010; Heo et al., 2011). Samples were observed with differential interference contrast optics using an Axio Imager.A1 microscope (Carl Zeiss), and then the digital images were obtained with the AxioCam MRc5 digital camera (Carl Zeiss) equipped on the microscope. For GFP visualization, the Fluoview FV300 (Olympus) confocal laser scanning microscope was used as described (Yu et al., 2010; Heo et al., 2011).

Transient Expression Assay

The protocol used for the transient expression assay, including protoplast preparation, transformation, and LUC activity measurement, is basically the same as that described previously (Yoo et al., 2007) with minor modifications. Protoplasts were prepared from rosette leaves of 3- to 4-week-old Col-0 plants using cellulose R10 and macerozyme R10 (Yakult Pharmaceutical). Transformation was performed using polyethylene glycol solution including 40% (w/v) polyethylene glycol 4000 (Fluka), 200 mM mannitol (Duchefa Biochemie), and 100 mM $CaCl_2$ (Sigma) in the presence of the effector and/or reporter plasmids for 5 min. The plasmids were prepared with the AxyPrep Maxi-Plasmid kit (Axygen), and a total of 10 μg of plasmid DNA was used at a ratio of 9:9:2 (effector:reporter:control). After transformation, protoplasts were incubated in the washing and incubation buffer (500 mM mannitol, 4 mM MES, and 20 mM KCl) in the absence or presence of 300 mM Glc at 22°C for 16 h in the dark. Harvested protoplasts were lysed and measured for LUC activity using the Dual-Luciferase Reporter Assay System (Promega). The reporter gene activity was normalized by *Renilla* LUC activity. Experiments were independently repeated three times for biological replicates.

Sequence data from this article can be found in The Arabidopsis Information Resource data libraries under accession numbers AT4G33520 (GIG/PAA1), AT3G18780 (ACTIN2), AT4G39210 (APL3), AT5G13930 (CHS), AT4G29130 (HXK1), AT1G16540 (ABI3), AT2G40220 (ABI4), and AT2G36270 (ABI5).

Supplemental Data

The following materials are available in the online version of this article.

Supplemental Figure S1. Analysis of the stem cell niche in Col-0 and *gig* roots.

Supplemental Figure S2. Comparative analysis of Col-0 and *gig* adult plants.

Supplemental Figure S3. Complementation of *gig* with Cu supplementation.

Supplemental Figure S4. Root growth assay in the absence or presence of Cu with increasing Glc concentrations.

Supplemental Figure S5. Expression analysis of Glc-responsive genes with the addition of Cu.

Supplemental Figure S6. Prediction of an ABA-responsive element sequence in the *GIG* promoter.

Supplemental Table S1. Sequence information of PCR primers used in this study.

ACKNOWLEDGMENTS

We thank Eun Shim Hong, Dong Sung Jang, Gyuree Kim, and Gyu Min Lee for technical assistance. We also thank the Arabidopsis Biological Resource Center and the Nottingham Arabidopsis Stock Centre for plant materials.

Received November 30, 2011; accepted May 10, 2012; published May 11, 2012.

LITERATURE CITED

Abdel-Ghany SE, Müller-Moulé P, Niyogi KK, Pilon M, Shikanai T (2005) Two P-type ATPases are required for copper delivery in *Arabidopsis thaliana* chloroplasts. Plant Cell **17:** 1233–1251

Acevedo-Hernández GJ, León P, Herrera-Estrella LR (2005) Sugar and ABA responsiveness of a minimal RBCS light-responsive unit is mediated by direct binding of ABI4. Plant J **43:** 506–519

Achard P, Gusti A, Cheminant S, Alioua M, Dhondt S, Coppens F, Beemster GT, Genschik P (2009) Gibberellin signaling controls cell proliferation rate in Arabidopsis. Curr Biol **19:** 1188–1193

Arenas-Huertero F, Arroyo A, Zhou L, Sheen J, León P (2000) Analysis of Arabidopsis glucose insensitive mutants, *gin5* and *gin6*, reveals a central role of the plant hormone ABA in the regulation of plant vegetative development by sugar. Genes Dev **14:** 2085–2096

Arroyo A, Bossi F, Finkelstein RR, León P (2003) Three genes that affect sugar sensing (*abscisic acid insensitive 4*, *abscisic acid insensitive 5*, and *constitutive triple response 1*) are differentially regulated by glucose in Arabidopsis. Plant Physiol **133:** 231–242

Baier M, Hemmann G, Holman R, Corke F, Card R, Smith C, Rook F, Bevan MW (2004) Characterization of mutants in Arabidopsis showing increased sugar-specific gene expression, growth, and developmental responses. Plant Physiol **134:** 81–91

Buchanan B, Gruissem W, Jones RL (2000) Biochemistry and Molecular Biology of Plants. American Society of Plant Biologists, Rockville, MD

Cheng WH, Endo A, Zhou L, Penney J, Chen HC, Arroyo A, Leon P, Nambara E, Asami T, Seo M, et al (2002) A unique short-chain

dehydrogenase/reductase in *Arabidopsis* glucose signaling and abscisic acid biosynthesis and functions. Plant Cell **14:** 2723–2743

Cho YH, Yoo S-D, Sheen J (2006) Regulatory functions of nuclear hexokinase1 complex in glucose signaling. Cell **127:** 579–589

Clough SJ, Bent AF (1998) Floral dip: a simplified method for Agrobacterium-mediated transformation of *Arabidopsis thaliana*. Plant J **16:** 735–743

Curtis MD, Grossniklaus U (2003) A Gateway cloning vector set for high-throughput functional analysis of genes in planta. Plant Physiol **133:** 462–469

Dekkers BJ, Schuurmans JA, Smeekens SC (2008) Interaction between sugar and abscisic acid signalling during early seedling development in Arabidopsis. Plant Mol Biol **67:** 151–167

Dello Ioio R, Linhares FS, Scacchi E, Casamitjana-Martinez E, Heidstra R, Costantino P, Sabatini S (2007) Cytokinins determine Arabidopsis root-meristem size by controlling cell differentiation. Curr Biol **17:** 678–682

Di Laurenzio L, Wysocka-Diller J, Malamy JE, Pysh L, Helariutta Y, Freshour G, Hahn MG, Feldmann KA, Benfey PN (1996) The *SCARECROW* gene regulates an asymmetric cell division that is essential for generating the radial organization of the Arabidopsis root. Cell **86:** 423–433

Donnelly PM, Bonetta D, Tsukaya H, Dengler RE, Dengler NG (1999) Cell cycling and cell enlargement in developing leaves of Arabidopsis. Dev Biol **215:** 407–419

Dugas DV, Bartel B (2008) Sucrose induction of Arabidopsis miR398 represses two Cu/Zn superoxide dismutases. Plant Mol Biol **4:** 403–417

Fey V, Wagner R, Braütigam K, Wirtz M, Hell R, Dietzmann A, Leister D, Oelmüller R, Pfannschmidt T (2005) Retrograde plastid redox signals in the expression of nuclear genes for chloroplast proteins of *Arabidopsis thaliana*. J Biol Chem **280:** 5318–5328

Finkelstein RR, Gibson SI (2002) ABA and sugar interactions regulating development: cross-talk or voices in a crowd? Curr Opin Plant Biol **5:** 26–32

Finkelstein RR, Wang ML, Lynch TJ, Rao S, Goodman HM (1998) The *Arabidopsis* abscisic acid response locus *ABI4* encodes an APETALA 2 domain protein. Plant Cell **10:** 1043–1054

Gallagher KL, Paquette AJ, Nakajima K, Benfey PN (2004) Mechanisms regulating SHORT-ROOT intercellular movement. Curr Biol **14:** 1847–1851

Gibson SI (2005) Control of plant development and gene expression by sugar signaling. Curr Opin Plant Biol **8:** 93–102

Helariutta Y, Fukaki H, Wysocka-Diller J, Nakajima K, Jung J, Sena G, Hauser MT, Benfey PN (2000) The *SHORT-ROOT* gene controls radial patterning of the Arabidopsis root through radial signaling. Cell **101:** 555–567

Heo JO, Chang KS, Kim IA, Lee MH, Lee SA, Song SK, Lee MM, Lim J (2011) Funneling of gibberellin signaling by the GRAS transcription regulator SCARECROW-LIKE 3 in the Arabidopsis root. Proc Natl Acad Sci USA **108:** 2166–2171

Huijser C, Kortstee A, Pego J, Weisbeek P, Wisman E, Smeekens S (2000) The Arabidopsis *SUCROSE UNCOUPLED-6* gene is identical to *ABSCISIC ACID INSENSITIVE-4*: involvement of abscisic acid in sugar responses. Plant J **23:** 577–585

Hwang I, Kim SY, Kim CS, Park Y, Tripathi GR, Kim SK, Cheong H (2010) Over-expression of the *IGI1* leading to altered shoot-branching development related to MAX pathway in Arabidopsis. Plant Mol Biol **73:** 629–641

Jeong SW, Das PK, Jeoung SC, Song JY, Lee HK, Kim YK, Kim WJ, Park YI, Yoo SD, Choi SB, et al (2010) Ethylene suppression of sugar-induced anthocyanin pigmentation in Arabidopsis. Plant Physiol **154:** 1514–1531

Jung HS, Chory J (2010) Signaling between chloroplasts and the nucleus: can a systems biology approach bring clarity to a complex and highly regulated pathway? Plant Physiol **152:** 453–459

Kim C, Lee KP, Baruah A, Nater M, Göbel C, Feussner I, Apel K (2009) $^1O_2$-mediated retrograde signaling during late embryogenesis predetermines plastid differentiation in seedlings by recruiting abscisic acid. Proc Natl Acad Sci USA **106:** 9920–9924

Kleine T, Voigt C, Leister D (2009) Plastid signalling to the nucleus: messengers still lost in the mists? Trends Genet **25:** 185–192

Koch KE (1996) Carbohydrate-modulated gene expression in plants. Annu Rev Plant Physiol Plant Mol Biol **47:** 509–540

Koussevitzky S, Nott A, Mockler TC, Hong F, Sachetto-Martins G, Surpin M, Lim J, Mittler R, Chory J (2007) Signals from chloroplasts converge to regulate nuclear gene expression. Science **316:** 715–719

Lee MH, Kim B, Song SK, Heo JO, Yu NI, Lee SA, Kim M, Kim DG, Sohn SO, Lim CE, et al (2008) Large-scale analysis of the GRAS gene family in *Arabidopsis thaliana*. Plant Mol Biol **67:** 659–670

Leister D, Wang X, Haberer G, Mayer KFX, Kleine T (2011) Intracompartmental and intercompartmental transcriptional networks coordinate the expression of genes for organellar functions. Plant Physiol **157:** 386–404

León P, Sheen J (2003) Sugar and hormone connections. Trends Plant Sci **8:** 110–116

Li Y, Lee KK, Walsh S, Smith C, Hadingham S, Sorefan K, Cawley G, Bevan MW (2006) Establishing glucose- and ABA-regulated transcription networks in Arabidopsis by microarray analysis and promoter classification using a Relevance Vector Machine. Genome Res **16:** 414–427

Liu YG, Mitsukawa N, Oosumi T, Whittier RF (1995) Efficient isolation and mapping of *Arabidopsis thaliana* T-DNA insert junctions by thermal asymmetric interlaced PCR. Plant J **8:** 457–463

Mita S, Murano N, Akaike M, Nakamura K (1997) Mutants of *Arabidopsis thaliana* with pleiotropic effects on the expression of the gene for β-amylase and on the accumulation of anthocyanin that are inducible by sugars. Plant J **11:** 841–851

Moore B, Zhou L, Rolland F, Hall Q, Cheng WH, Liu YX, Hwang I, Jones T, Sheen J (2003) Role of the Arabidopsis glucose sensor HXK1 in nutrient, light, and hormonal signaling. Science **300:** 332–336

Nakajima K, Sena G, Nawy T, Benfey PN (2001) Intercellular movement of the putative transcription factor SHR in root patterning. Nature **413:** 307–311

Nott A, Jung HS, Koussevitzky S, Chory J (2006) Plastid-to-nucleus retrograde signaling. Annu Rev Plant Biol **57:** 739–759

Oswald O, Martin T, Dominy PJ, Graham IA (2001) Plastid redox state and sugars: interactive regulators of nuclear-encoded photosynthetic gene expression. Proc Natl Acad Sci USA **98:** 2047–2052

Palmer CM, Guerinot ML (2009) Facing the challenges of Cu, Fe and Zn homeostasis in plants. Nat Chem Biol **5:** 333–340

Penfield S, Li Y, Gilday AD, Graham S, Graham IA (2006) *Arabidopsis* ABA INSENSITIVE4 regulates lipid mobilization in the embryo and reveals repression of seed germination by the endosperm. Plant Cell **18:** 1887–1899

Pfannschmidt T (2010) Plastidial retrograde signalling: a true "plastid factor" or just metabolite signatures? Trends Plant Sci **15:** 427–435

Pogson BJ, Woo NS, Förster B, Small ID (2008) Plastid signalling to the nucleus and beyond. Trends Plant Sci **13:** 602–609

Priest HD, Filichkin SA, Mockler TC (2009) *Cis*-regulatory elements in plant cell signaling. Curr Opin Plant Biol **12:** 643–649

Ramon M, Rolland F, Sheen J (2008) Sugar sensing and signaling. The Arabidopsis Book. **6:** e0117, doi/10.1199/tab.0117

Rolland F, Baena-Gonzalez E, Sheen J (2006) Sugar sensing and signaling in plants: conserved and novel mechanisms. Annu Rev Plant Biol **57:** 675–709

Rook F, Bevan MW (2003) Genetic approaches to understanding sugar-response pathways. J Exp Bot **54:** 495–501

Sabatini S, Heidstra R, Wildwater M, Scheres B (2003) SCARECROW is involved in positioning the stem cell niche in the Arabidopsis root meristem. Genes Dev **17:** 354–358

Sarkar AK, Luijten M, Miyashima S, Lenhard M, Hashimoto T, Nakajima K, Scheres B, Heidstra R, Laux T (2007) Conserved factors regulate signalling in *Arabidopsis thaliana* shoot and root stem cell organizers. Nature **446:** 811–814

Scheres B (2007) Stem-cell niches: nursery rhymes across kingdoms. Nat Rev Mol Cell Biol **8:** 345–354

Shen YY, Wang XF, Wu FQ, Du SY, Cao Z, Shang Y, Wang XL, Peng CC, Yu XC, Zhu SY, et al (2006) The Mg-chelatase H subunit is an abscisic acid receptor. Nature **443:** 823–826

Shikanai T, Müller-Moulé P, Munekage Y, Niyogi KK, Pilon M (2003) PAA1, a P-type ATPase of *Arabidopsis*, functions in copper transport in chloroplasts. Plant Cell **15:** 1333–1346

Smeekens S (2000) Sugar-induced signal transduction in plants. Annu Rev Plant Physiol Plant Mol Biol **51:** 49–81

Solfanelli C, Poggi A, Loreti E, Alpi A, Perata P (2006) Sucrose-specific induction of the anthocyanin biosynthetic pathway in Arabidopsis. Plant Physiol **140:** 637–646

Strand A, Asami T, Alonso J, Ecker JR, Chory J (2003) Chloroplast to nucleus communication triggered by accumulation of Mg-protoporphyrinIX. Nature **421:** 79–83

Sunkar R, Kapoor A, Zhu JK (2006) Posttranscriptional induction of two Cu/Zn superoxide dismutase genes in *Arabidopsis* is mediated by downregulation of miR398 and important for oxidative stress tolerance. Plant Cell **18:** 2051–2065

Teng S, Keurentjes J, Bentsink L, Koornneef M, Smeekens S (2005) Sucrose-specific induction of anthocyanin biosynthesis in Arabidopsis requires the *MYB75/PAP1* gene. Plant Physiol **139:** 1840–1852

Tsukagoshi H, Busch W, Benfey PN (2010) Transcriptional regulation of ROS controls transition from proliferation to differentiation in the root. Cell **143:** 606–616

Tsukaya H, Ohshima T, Naito S, Chino M, Komeda Y (1991) Sugar-dependent expression of the *CHS-A* gene for chalcone synthase from petunia in transgenic Arabidopsis. Plant Physiol **97:** 1414–1421

Ubeda-Tomás S, Federici F, Casimiro I, Beemster GT, Bhalerao R, Swarup R, Doerner P, Haseloff J, Bennett MJ (2009) Gibberellin signaling in the endodermis controls Arabidopsis root meristem size. Curr Biol **19:** 1194–1199

Weigel D, Ahn JH, Blázquez MA, Borevitz JO, Christensen SK, Fankhauser C, Ferrándiz C, Kardailsky I, Malancharuvil EJ, Neff MM, et al (2000) Activation tagging in Arabidopsis. Plant Physiol **122:** 1003–1013

Williams LE, Mills RF (2005) $P_{(1B)}$-ATPases: an ancient family of transition metal pumps with diverse functions in plants. Trends Plant Sci **10:** 491–502

Xiao W, Sheen J, Jang JC (2000) The role of hexokinase in plant sugar signal transduction and growth and development. Plant Mol Biol **44:** 451–461

Yamasaki H, Abdel-Ghany SE, Cohu CM, Kobayashi Y, Shikanai T, Pilon M (2007) Regulation of copper homeostasis by micro-RNA in Arabidopsis. J Biol Chem **282:** 16369–16378

Yoo SD, Cho YH, Sheen J (2007) Arabidopsis mesophyll protoplasts: a versatile cell system for transient gene expression analysis. Nat Protoc **2:** 1565–1572

Yu NI, Lee SA, Lee MH, Heo JO, Chang KS, Lim J (2010) Characterization of SHORT-ROOT function in the Arabidopsis root vascular system. Mol Cells **30:** 113–119

Yuan K, Wysocka-Diller J (2006) Phytohormone signalling pathways interact with sugars during seed germination and seedling development. J Exp Bot **57:** 3359–3367